9-1. Research Divisions
Division for Meteorological and Atmospheric Research

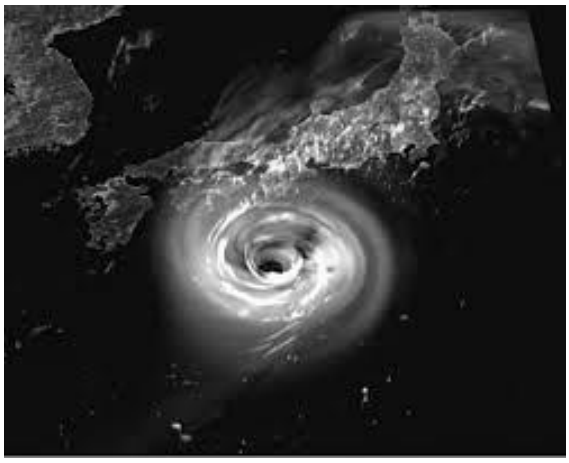

Research topics and keywords

- Millimeter-wave/infrared interferometry of trace gases such as greenhouse gases and ozone depleting substances
- Precipitation measurements by advanced polarimetric radars and hydrometeor videosondes
- Laser/optical measurements and chamber data analysis of trace gases and aerosol properties
- Development of new instrumental technology
- Development of a numerical cloud model (CReSS) and meteorological studies with numerical simulations
- Clouds and precipitation observed by multiple satellites

Introduction to Division for Meteorological and Atmospheric Research

Ongoing global warming caused by increasing concentrations of carbon dioxide and other greenhouse gases will result in both gradual climate change and intensification of weather extremes and ecological catastrophes. Among the most urgent tasks for confronting global environmental problems more effectively is close monitoring of the atmosphere using different observation methods and a better understanding of the atmosphere through theoretical insights and numerical modeling. To address these problems, the Division for Meteorological and Atmospheric Research is dedicated to a number of research projects for exploring the atmosphere from a range of different angles.

Main Achievements in FY2017

1. Characteristics of a positive K_{DP}-peak layer above the melting level in a stratiform region observed by Ka-band radar and balloon-borne particle observation

Ka-band polarimetric radar is sensitive to the number and shape of ice crystals. A simultaneous observation using C- and Ka-band polarimetric radars and balloon-borne particle soundings, videosondes (VS) and Hydrometeor Videosondes (HYVIS), was conducted at Okinawa Island, Japan, in June 2016. A positive K_{DP}-peak layer between 6.0 and 7.5 km above the melting level in a stratiform region associated with the Baiu front was observed by the Ka-band radar during the VS and HYVIS observations on June 3. The maximum K_{DP} value reached 2.5 deg./km in the layer, although that above and below the layer was less than 1.0 deg./km. The layer extended over 20 km in the horizontal direction; however, the positive K_{DP}-peak was not observed by the C-band radar at that time.

An approximate formula for K_{DP} for oblate ice crystals provides a K_{DP} value dependent on the axis ratio, the equal-volume spherical diameter, and the number concentration of particles. The vertical profile of K_{DP} at every 250 m-height step was estimated using VS data and the approximate formula. The estimated K_{DP} profile reproduced the observed profile well, including the positive K_{DP}-peak layer. The axis ratio is approximately constant in the positive K_{DP}-peak layer and suggests the existence of plate- and/or column-type ice crystals. The number concentration of ice crystals has a clear peak corresponding to the positive K_{DP}-peak layer, indicating that the positive K_{DP}-peak can be attributed to the large number of plate and/or column-type ice crystals. The VS and HYVIS observations show the existence of a small number of snow-aggregates between the positive K_{DP}-peak layer and the melting level. K_{DP} values below the peak level can be attributed to the aggregation of ice crystals.

2. Possibility of particle identification in solid hydrometeors using Ka-band polarimetric radar

To clarify the relationship between the polarimetric parameters obtained using Ka-band radar and the characteristics of solid hydrometeors in snow clouds, we installed a Ka-band polarimetric radar at Ishikawa Prefectural University in the winter season of

2016–2017. We also installed a PARSIVEL that can observe the size, number, and fall speed of hydrometeors at Kanazawa University, located within the radar observation range. Here, the objective was to identify particles in solid hydrometeors using the polarimetric parameters (Z_H, Z_{DR}, K_{DP}) obtained by the Ka-band radar. Using the PARSIVEL data, we calculated the center of mass flux (CMF) every 1 min to categorize dominant precipitation particles. The periods of the dominant particles were divided into graupel-dominant, snowflake-dominant, and crystal-dominant periods using the CMF. The target region was set as a "circular sector" wherein particles are expected to reach the PARSIVEL observation point based on the movement direction and speed of the echo pattern. A total of 78 scanning data from the snowfall event observed on January 24 and 25, 2017, were analyzed. During the snowflake-dominant period, moderate numbers of crystals and snowflakes were detected by PARSIVEL. The positive spread in the probability density functions (PDFs) of Z_{DR} and K_{DP} in the target region was analyzed, corresponding to previous studies using X-band polarimetric radars. A large number of crystals and graupel particles co-exist during the graupel-dominant period, and the PDFs of Z_{DR} and K_{DP} were wide with both positive and negative components. However, there were no clear differences between the PDFs of Z_{DR} and K_{DP} between the graupel- and snowflake-dominant periods; hence, particle identification in solid hydrometeors using polarimetric parameters obtained by Ka-band radar is likely to be difficult.

3. Cloud radar observation for the initial development stage of summer cumulonimbus clouds

During summer in Japan, atmospheric stratification becomes unstable due to heating from the ground surface under strong solar radiation. Isolated convective clouds are frequently generated without large-scale disturbance; some of these convective clouds are highly developed and cause intense precipitation over short time periods. In contrast, many convective clouds disappear without development. To examine the characteristics of the initial development stage of highly developed cumulonimbus clouds, we conducted an observation using a Nagoya University cloud radar during the summer of 2017 in Kobe. The cloud radar is capable of detecting small cloud particles using a shorter wavelength (Ka band) than the more widely used precipitation radar, with high spatial resolution. The observation results suggested that there was a significant difference in the organization of convective cells between developed and undeveloped convective clouds. This observation project was conducted using a range of instruments in collaboration with other research institutions, and will be continued in the next fiscal year.

4. Development of MP-PAWR and analysis of a tornado event using PAWR

Under the CSTI's SIP program, a dual polarization multi-parameter phased array weather radar (MP-PAWR) was developed in cooperation with NICT, Tokyo Metropolitan University, the Toshiba Corporation and Nagoya University. Since MP-PAWR can provide denser 3-D data with a temporal resolution 10 times greater than that of conventional weather radar, it can be used to observe rapidly changing clouds such as torrential rain and tornadoes. A cumulonimbus cloud that brought a waterspout in Okinawa Prefecture was analyzed using single polarized phased array weather radar (PAWR) as a preliminary study for MP-PAWR. The cumulonimbus cloud was observed both by the KIN radar from Nagoya University located at the University of the Ryukyus and the PAWR located at NICT. In this analysis, a miso-scale vortex with a diameter of 1 to 2 km corresponding to a hook echo was observed, and the PAWR data revealed the detailed vertical extent of the miso-cyclone with high temporal resolution.

5. Radiative regulation of tropical convection by preceding cirrus clouds

Radiative-convective interactions, although known to be a critical physical element of the Earth's atmosphere, are not understood in the context of the development of individual convective systems. This work targeted evidence of convective-radiative interactions in satellite measurements, with a focus on the variability over the life cycle of tropical convection. To this end, the vertical profiles of cloud cover and radiative heating from the CloudSat-CALIPSO products were sorted into a composite time series around the hours of convective occurrence identified by TRMM PR. Cirrus cloud cover begins to increase, accompanied by a notable reduction in LW cooling, in moist atmospheres even 1–2 days before deep convection is invigorated. In contrast, LW cooling stays efficient and clouds remain shallow where the ambient air is very dry. A possible mechanism to support this observation was discussed using a simple conceptual model. The model

suggests that the preceding cirrus clouds could radiatively promote moistening with the aid of congestus-mode (or a vertical mode with a lower-tropospheric updraft) dynamics within a short period of time (about 2 days), as observed.

6. Monitoring of stratospheric ozone, UV, and aerosols in the Patagonia region, South America

We have continued a joint research project with Argentina and Chile called "Development of the Atmospheric Environmental Risk Management System in South America", as part of the SATREPS program operated by the Japan Science and Technology Agency (JST) and the Japan International Cooperation Agency (JICA). In 2017, we developed a risk information platform called GeoUV that provides UV forecasting and real-time UV data obtained from 36 stations located over Chile and Argentina. In addition, development of an aerosol lidar network that consists of nine lidars spread over the two countries has been completed in collaboration with the National Institute for Environmental Studies (NIES).

To forecast the influence of the ozone hole on the southern tip regions of South America, we conducted comparative experiments with two ozone prediction models in collaboration with the model analysis group at NIES. One is a chemical transport model nudged towards the meteorological forecast data provided by NCEP/GFS (model 1), and the other is a chemical climate assimilation mode using a local ensemble transform Kalman filter (model 2). The model results show good agreement with the observed data from OMI, within ±10 DU for 1-week forecasts and ±20 DU for 10-day forecasts, from models 1 and 2, respectively.

Fluctuations of ozone (O_3) concentrations with dimensions of a few kilometers, so-called O_3 laminae, were identified in the southern tip region during the 4th campaign observation in 2016. In 2017, we conducted a statistical analysis using the archived ozonesonde measurements from after 2008 and meteorological reanalysis data MERRA2/NASA to clarify the relationship between O_3 laminae and atmospheric waves. We found that Rossby wave–induced variability accounts for a larger proportion of the observed variability than gravity wave-induced variability in this region. We also found that the effect of Rossby waves is more significant inside the polar vortex than outside or near the edge of the polar vortex in the stratosphere, in the period between June and November.

7. Observations of chemical composition changes in the polar mesosphere

Due to the magnetic field configuration, the polar mesosphere is a region where energetic particle precipitation (EPP) events trigger a series of ion-molecule chemical reactions caused by ionization and dissociation of nitrogen and oxygen molecules, and affect the atmospheric composition. To understand these processes more fully, the ISEE and the NIPR conducted continuous monitoring of nitric oxide (NO) and O_3 concentrations in the mesosphere and lower thermosphere using a ground-based millimeter-wave spectral radiometer from January 2012 onwards. During a geomagnetic storm event in April 2017, we detected a fourfold enhancement of the NO column density, and also found that the annual variation of the NO column has exhibited a gradual decrease in amplitude since 2015.

Measurements with the millimeter-wave spectral radiometer installed at Tromsø, Norway, in collaboration with the University of Tromsø are suspended because of an abnormal increase in the room temperature, and snow cover to the skylight. We have installed a warm air system at the container and confirmed that it works well. Simultaneous measurements of NO in Syowa and Tromsø will start again in the 2018 season.

8. Long-term monitoring of tropospheric and stratospheric minor constituents using a high-resolution Fourier-Transform InfraRed (FTIR) spectrometer at Rikubetsu

Measurements of atmospheric trace gases in the troposphere and stratosphere with ground-based high-resolution FTIR instruments (Bruker IFS120 M up to 2010 and Bruker IFS120/5HR since 2014) have been conducted since 1995 as part of the Network for the Detection of Atmospheric Composition Change (NDACC). A solar absorption spectrum is obtained with six optical filters in the 2–15 μm region with a resolution of 0.0035 cm^{-1}, and the vertical distribution of trace gases is retrieved from the measured spectrum using the SFIT4 (version 0.944) software with the uniform retrieval parameters recommended by NDACC. Total column amounts and vertical profiles of O_3, HCl, HF, HNO_3, $ClONO_2$, CH_4, C_2H_6, N_2O, CO, HCN and CCl_4 are observed,

and their temporal variations and long-term trends from 1995 to 2016 have been obtained. The observed partial column of stratospheric O_3 does not show any significant trend, although that in the troposphere seemed to decrease in the 2000s. Negative trends were observed in the time series of the HCl and $ClONO_2$ columns since 2000, consistent with global results. Significant enhancement of HCN in the lower stratosphere from 1998 to 2001 was also observed, and a trajectory analysis suggested that this was not affected by transport of a polluted air mass following the huge biomass burning event in Indonesia in 1997.

9. Development of a wide frequency range and dynamic range detector for a new radiometer system

Recently, millimeter-terahertz band technologies for application to information, telecommunications and radio astronomy research have developed rapidly. We are developing a new receiver system for our atmospheric radiometers that is wide-band, highly sensitive and highly accurate based on these new technologies. This year, we have developed a superconducting tunnel junction (SIS) device and a multiplexer in the 200 GHz band through collaborative research with the Advanced Technology Center (ATC) at the National Astronomical Observatory of Japan (NAOJ) and NICT, respectively. We have successfully fabricated SIS devices in a clean room at the ATC, and started measurement of the performance of these devices. The multiplexer is a waveguide component for observation of multi-line atmospheric molecules (O_3, NO_x, HO_x and ClO_x) in Antarctica. At NICT, we have fabricated a waveguide circuit for the multiplexer by metal cutting, and measured the transmission characteristics with a mm-band network analyzer at NICT. This result correlated well with a 3D electromagnetic field simulator, and we have proved the validity of our waveguide circuit design.

10. Measurement of column-averaged molar mixing ratios of CO_2 using a portable spectrometer in Tokyo

We measured the daytime column-averaged dry-air molar mixing ratios of atmospheric CO_2 and XCO_2 in the central area of Tokyo between September 2014 and August 2016 using a portable optical spectrometer. The observed seasonal cycle was compared with that from the TCCON site in Tsukuba, 60 km northeast of Tokyo. The seasonal variation of XCO_2 at the Tsukuba site has maxima around March-April and minima in August-September. In contrast, the seasonal variations of XCO_2 at the Tokyo site reach maxima in December–January and minima in July–August. There are large differences in XCO_2 concentrations between the two different sites (~5 ppm) in December–February; however, these differences are smaller (~0.5 ppm) in June–September, probably due to large anthropogenic emissions of CO_2 from heating, especially in winter in the Tokyo metropolitan area.

11. Observation of $PM_{2.5}$ using low-cost optical sensors in Asian countries

Fine particulate matter such as $PM_{2.5}$ has negative impacts on human health, causing heart disease, stroke, lung cancer and chronic obstructive pulmonary disease, resulting in premature mortality. We have developed a new palm-sized optical $PM_{2.5}$ sensor with the Panasonic Corporation. The $PM_{2.5}$ mass concentrations obtained by this sensor correlate well with corresponding data obtained by large beta-attenuation monitors in many places. The $PM_{2.5}$ sensor has been used for observation in Asian countries, including Hanoi in Vietnam, New Delhi in India, and Ulaanbaatar in Mongolia. In both New Delhi and Ulaanbaatar, very high concentrations of $PM_{2.5}$ of over 1000 $\mu g/m^3$ were observed in winter, probably due to emissions from combustion processes such as burning of agricultural residues and combustion for heating/cooking.

12. Observation of ozone-induced potential aerosol formation in a suburban forest

Secondary organic aerosol (SOA) particles, which are generated during oxidation of volatile organic compounds (VOCs), constitute a large fraction of submicron particles. However, the formation processes of SOA remain largely uncertain. As a new approach to investigating their formation processes, ozone-induced potential aerosol formation was measured in summer at a suburban deciduous forest near Tokyo. After passage through a reactor containing high concentrations of ozone, increases in total particle volume were observed; however, the model simulation could explain only ~40% of the observed particle formation, and large discrepancies were found, especially during the daytime when the concentrations of isoprene and oxygenated VOCs were high. The results suggest a significant contribution from missing SOA formation processes from VOCs, especially those emitted during the daytime.